An Arrangement of Ideal Reactors as a Way to Model Homogenizing Processes with a Planetary Mixer

Guillaume Delaplace, Laurent Bouvier, and Anne Moreau
INRA, UR 638, F-59650, Villeneuve d'ascq Cedex, France

Christophe Andre
Hautes Etudes d' Ingénieur (H.E.I.), Laboratoire de Génie de Procédés, 59046 Lille, France

DOI 10.1002/aic.12384
Published online August 23, 2010 in Wiley Online Library (wileyonlinelibrary.com).

This article investigates ways of modeling the homogenization mechanism occurring when mixing highly viscous Newtonian fluids with a planetary mixer. In particular, an arrangement of ideal reactors containing a perfect-mixed zone sweeping out a torus reactor is proposed to represent the dynamics of the mixing process. The originality of the arrangement of ideal reactors developed is due to the time–dependent location of the perfect-mixed zone in the torus which mimics the periodic revolution motion of the agitator around the vertical and central axis in the vessel. To ascertain the reliability of the method proposed, tracer injections were carried out with a planetary mixer named TRIAXE® system. It is shown that modeling results are in close agreement with experimental ones on the whole range of impeller revolution speeds tested. The model proposed captures well the physical mixing phenomena. © 2010 American Institute of Chemical Engineers *AIChE J,* 57: 1678–1683, 2011
Keywords: mixing, highly viscous fluids, planetary mixers, flow modeling

Introduction

High-viscosity mixing operations in batch mode are commonly encountered in chemical and food industries. Since batch mixing operations are both time and energy consuming, their optimization remains an important challenge for process engineers.

From a technological standpoint, this optimization is sought by introducing mixers that combine several movements. The TRIAXE® is a mixing equipment which has been designed with this goal. Good overall homogenization performances obtained with the TRIAXE® system may be explained by the dual motions of the impeller. On one hand, the rotation allows high shearing to be imparted to the fluid in the gap between the blade and the vessel wall. On the other hand, gyration enables the agitator to visit the entire volume of the fluid and renewal of the fluid in the vicinity of the blade.

From the academic point of view, this optimization is sought through better knowledge of the velocity field. Current knowledge is still limited for providing straightforward solutions to obtain the velocity field of an agitator combining dual revolutionary motions even for the laminar regime. Moreover, when commercial computational fluid dynamic software succeeds in delivering this goal with high engineering effort, computational time is too long.

When such information upon the flow field is not available, an alternative solution to predict mixing time evolution with impeller speeds is to model mixing equipment by a network of ideal reactors. Networks of ideal reactors have been used since the 1960s to model residence time distribution[1] with continuous reactor and then mixing process with classical agitator in batch (centrally and vertically mounted in the

This work was presented in SFGP 2009 in Marseille.
Correspondence concerning this article should be addressed to G. Delaplace at guillaume.delaplace@lille.inra.fr.

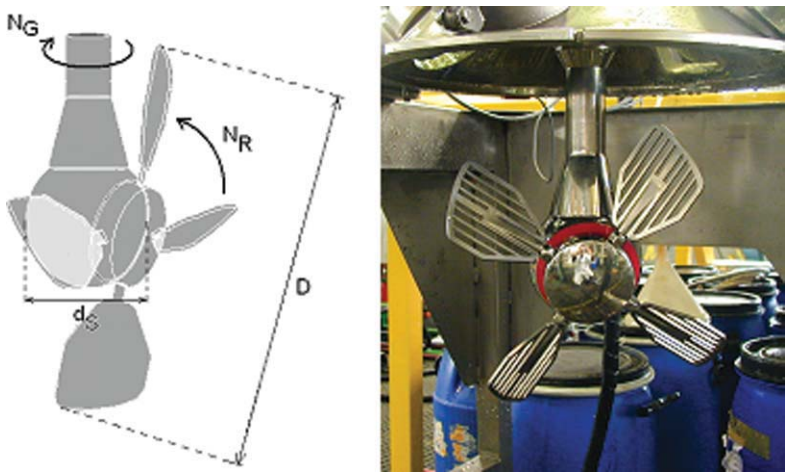

Figure 1. Diagram of the TRIAXE® system investigated *D* = 0.38 *m* and *ds* = 0.14 *m* (left). Picture of the impeller investigated (right).

[Color figure can be viewed in the online issue, which is available at wileyonlinelibrary.com.]

tank under steady stirring conditions). This has allowed us to obtain guidelines as to how the impeller rotational speeds influence mixing times in numerous reactors and succeed in modeling deviation from ideality for real reactor (channeling, recycling, creation of stagnant zone…). More recently, it has been shown that network of ideal reactors is a robust method which can even be applied to predict the mixing time under unsteady stirring conditions. Bearing that in mind a model based on an arrangement of ideal zones with shifting boundaries has been proposed to describe the flow in a vessel agitated by a PARAVISC® system.[2]

Unfortunately, this kind of approach has seldom been applied to reactors equipped with nonconventional agitators such as planetary mixers. However, these mixing equipments are common in some process industries such as dough manufacturer. The analysis of their performance characteristics have only recently appeared in open literature.[3–9] Therefore, it is needed to extend these approaches to planetary mixers to:

(1) deliver a model which can describe the combined effects of the dual impeller speed on mixing processes

(2) propose a control law concerning this impeller speed ratio for optimizing mixing processes.

This goal has been the main motivation for this work. In the following section, we will give more details about the mixing equipment, the tracer experiments, the arrangement of reactors and automaton proposed to mimic the dynamic of the mixing process. In particular, the experimental mixing runs required for the parameter estimation will be presented and discussed.

Material and Methods

Mixing equipment

The mixer used in this work was a TRIAXE® system (TriaProcess, France), which allowed the agitator to combine two motions: gyration and rotation (Figure 1). Gyration is a revolution of the agitator around a vertical axis while rotation is a revolution of the agitator around a nearly horizontal axis. The dual motion allowed the agitator to sweep the entire volume of the vessel. More precisely, the mixing tool of the TRIAXE® system was a pitched four-blade turbine. Note that the particularity of this planetary mixer was that the axes of the two revolutionary motions were nearly perpendicular. The mixing equipment was driven by two variable speed motors. The mixing vessel was a transparent glass cylinder with rounded bottoms, which allowed to observe the dynamics of the mixing process. For all the experiments, the volume of liquid was maintained to 0.03 m^3.

Mixing runs and mixing times determination

Tracer injections were carried out for various ratios of gyrational and rotational speeds and reported in Table 1. The name of the run is indicated in the second column of Table 1 and is a rough indication of impeller speed ratios For example, G10R30 refers to a mixing process performed with a gyration and a rotation speed equal to 10% and 30% of their full speed range, respectively, available on each motor.

In Table 1, the viscosity of the Newtonian fluid tested (glucose syrup solution) at the temperature encountered in the vessel is given. For this liquid, the power and mixing curves given in the previous article have shown that the flow regime is laminar.[8–10] For each run, a colorimetric diagnosis was applied based on the image analysis captured by the webcam. More details about the tracer injection and colorimetric diagnosis are given elsewhere.[9-11] In this work, we used the evolution of the level of brightness of the green color *S*, captured on a digital image representing the tank, to reconstruct the homogenization progress. These values were normalized to obtain a rate of homogenization varying from zero to one to be compared with the normalized average spatial homogeneity, which evolves also from zero to one at the same time.

The normalized spatial homogeneity was the following:

$$\frac{S - S_0}{S_\infty - S_0} \tag{1}$$

Table 1. Operating Conditions and Mixing Time Obtained from Tracer Injection and Mixing Experiments

	Run Names	Gyration Speed N_G (s^{-1})	Rotation Speed N_R (s^{-1})	Viscosity (Pa s)	$t_{m90\%}$ (s)
Used for parameter identification	G50R10	0.15	0.17	23.6	157
	G50R50	0.15	0.74	18.0	69
	G50R70	0.15	1.05	17.4	89
	G50R90	0.15	1.44	31.7	42
Used to ascertain validity of the model	G40R70	0.12	1.03	23.3	61
	G70R30	0.23	0.50	17.6	82
	G70R50	0.23	0.78	18.4	73
	G70R70	0.23	1.10	25.1	68
	G70R90	0.23	1.49	22.4	44
	G90R10	0.32	0.27	13.8	93
	G90R30	0.32	0.55	17.2	75
	G90R70	0.32	1.15	15.7	62
	G90R90	0.32	1.54	14.4	33

In Eq. 1, S is the level of brightness of the green color at time t deduced from the tank image processing; S_0 and S_∞ are, respectively, initial and final values.

Reliability and repeatability of the video-imaging of colorization-decoloratization process (fast acid-base indicator reaction) in a mixer and the use of image analysis for describing the mixing progress have also been recently discussed in Cabaret et al.[12]

The mixing time was also extracted from colorimetric diagnosis and defined as the time between the injection zone and the time required to achieve a predetermined minimum deviation of 10% compared with the mean level of brightness for the green color. The injection was performed just before the arrival of the agitator in the injection zone.

Arrangement of ideal reactors proposed to describe the homogenization process investigated

Consider that the torus plotted in Figure 2 represents a top view of the real mixing equipment. It is assumed that the torus volume V is equal to the volume of the Newtonian liquid contained in the experimental tank.

The sketch represents a torus reactor divided into elementary control volumes. The bold line stands for perfect-mixed zone at initial position sliding in the torus at an angular gyrational speed equal to $2\pi \cdot N_G$ (N_G is given in s^{-1}). The dashed lines represent the next step position of the perfect-mixed zone.

This torus contains a perfect-mixed zone which slides in the torus reactor at a constant angular gyrational speed equal to $2\pi \cdot N_G$. The perfect-mixed zone is supposed to represent the action of the agitator blades on the liquid media. Indeed, it is assumed that the agitator blades create a perfect-mixed zone which periodically sweeps out and homogenizes the tank. The volume of the perfect-mixed zone $V_{\text{mixed zone}}$ is linked to the whole volume of the liquid in the tank, V by the above equation:

$$V = V_{\text{mixed zone}} + V_{\text{adj}} \tag{2}$$

In Eq. 2, V_{adj} represents the volume of the torus reactor which is not overlapped by the perfect-mixed zone.

In the arrangement of ideal reactors proposed, it is assumed that the volume of the perfect-mixed zone depends on the mixing intensity and is consequently dependent on the impeller rotational speed around the horizontal axis, N_R (s^{-1}).

Discretization and mass–balance applied in arrangement of ideal reactor to obtain the evolution with time of local tracer concentration in the torus reactor

Consider now that the torus volume is discritized into a finite number of elementary volumes, n. Each of these elementary volumes is assumed to be equal.

A small part of these control volumes, n_{mix} constitutes the perfect-mixed zone in which the tracer is instantaneously homogenized. Consequently ($n - n_{\text{mix}}$) represents the number of compartments which are not overlapped by the perfect-mixed zone and in which no homogenization occurs.

Considering now that Δt is an interval of time corresponding to the period required by the perfect-mixed zone for moving to the next and adjacent volume control. The consequence of this elementary movement is that the well-mixed zone overlaps a new previously adjacent compartment and contributes to homogenizing the viscous media.

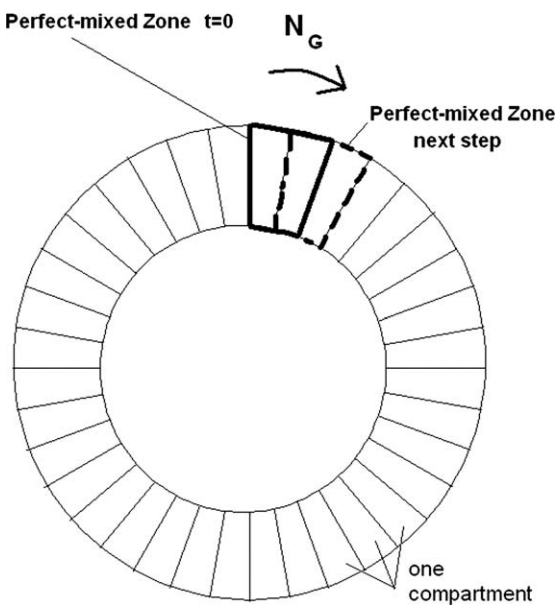

Figure 2. Arrangement of ideal reactors proposed.

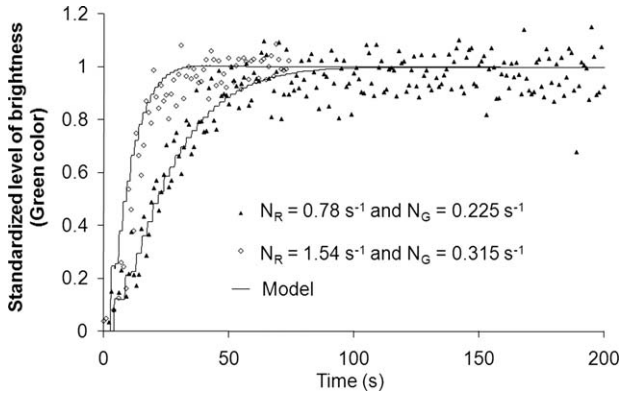

Figure 3. Examples of fitting allowing us to deduce volume of well-mixed zone.

A mass balance between t and $t + \Delta t$ in the well-mixed zone can consequently be expressed by:

$$C_{\text{mixed zone}}(t+\Delta t) = \frac{(n_{\text{mix}} - 1).C_{\text{mixed zone}}(t) + C_{\text{adj}}(t)}{n_{\text{mix}}} \quad (3)$$

$C_{\text{adj}}(t)$ is the tracer concentration reached in the adjacent cell located on the front edge of the perfect-mixed zone at time t.

On the contrary, the concentration in the compartment deserted by the perfect-mixed zone is kept unchanged preserving its previous value till it is swept out again by a next loop of the sliding perfect-mixed zone.

More details about the step by step computation of local concentration evolution with time is given in Appendix.

Thus, from the knowledge of initial and boundary conditions, it is easy for an automaton to obtain the evolution with time of the tracer concentration for each compartment constituting the torus and thus to simulate the evolution of the average spatial concentration obtained in a selected area of the real tank.

In our experiments: the initial conditions were the following: at time $t = 0$, a quantity of tracer is injected in a zone corresponding to the perfect-mixed zone (i.e., the initial position of the impeller). In all the other control volumes, the tracer concentration is set equal to zero. To ascertain the numerical results obtained by the proposed automaton with experimental ones, we have chosen to compare the progress of the normalized average spatial concentration $\overline{C}_{\text{normalized}}$ observed in a chosen part of the tank, V_{observed}.

$$\overline{C}_{\text{normalized}} = \frac{\overline{C}(t) - \overline{C}(0)}{\overline{C}(t=\infty) - \overline{C}(0)} \quad (4)$$

with

$$\overline{C} = \frac{\sum V_i.C_i}{V_{\text{observed}}} \text{ with } \quad 1 \le i \le n \quad (5)$$

In our experiments, V_{observed} corresponds to half of the torus. Experimentally, the tracer concentration in half of the tank was obtained by measuring the colorimetric distribution monitored by a webcam located in front of the tank.

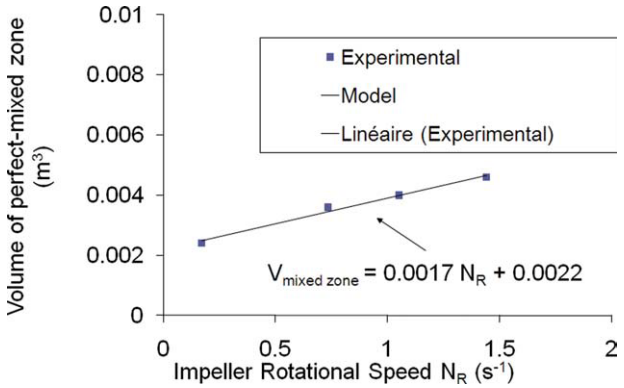

Figure 4. Evolution of the volume of the perfect-mixed zone with the impeller rotational speed.

[Color figure can be viewed in the online issue, which is available at wileyonlinelibrary.com.]

Results

Parameter identification

As mentioned before, preliminary tracer experiments have been necessary to determine the volume of the perfect-mixed zone and its evolution with impeller rotational speed. To make these identification tests, it was chosen to operate at constant impeller gyrational speed and various impeller rotational speeds and to attempt to adjust the volume of the well-mixed zone so that the mixing curves are described by the model. Figure 3 shows us an example of such a fitting. The tests used for identification are indicated in Table 1.

All the values of the volume of perfect-mixed zone identified in such a way are plotted vs. impeller rotational speed in Figure 4.

Figure 4 shows that as expected the volume of the perfect-mixed zone is an increasing function of the impeller rotational speed N_R (s^{-1}). This trend captures the fact that for a fixed impeller gyrational speed, the mixing process is faster when high impeller rotational speed is used. At this stage, the model is quite physical since it is expected that the well-mixed zone volume is dependent on the magnitude of impeller rotational speed.

For the range of operating conditions tested, it can also be observed that a linear regression gives an accurate estimation

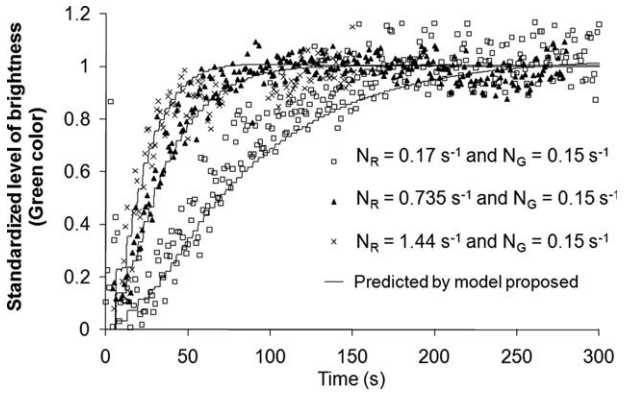

Figure 5. Influence of the impeller speed ratios on mixing times.

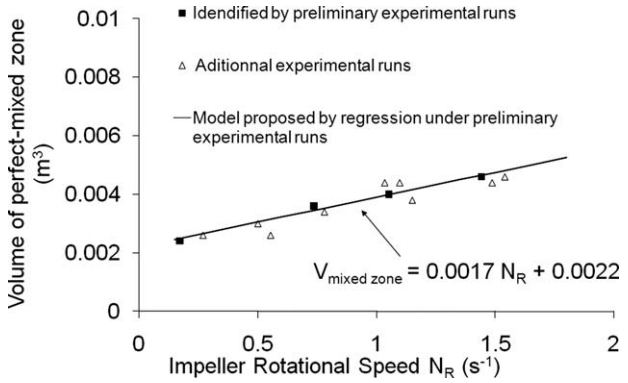

Figure 6. Evolution of the volume of the perfect-mixed zone for all experiments.

of the evolution of perfect-mixed zone volume with impeller rotational speed. Indeed:

$$V_{\text{mixed zone}} = 0.0017\ N_R + 0.0022 \tag{6}$$

In Eq. 6, N_R is given in s^{-1} and $V_{\text{mixed zone}}$ in m^3.

Reliability of the model

Using other operating conditions than those adopted for parameters estimation, the validity of the model was tested.

The performances of the model to describe the mixing process have been discussed with respect to their fitting agreement with the experimental curve when the volume of the perfect-mixed zone was predicted by Eq. 6.

An example of such comparison between experimental and simulated data is given in Figure 5.

Figure 5 shows that the predicted homogenization curve describes well the dynamic of the homogenization process whatever the stirring conditions adopted. This agreement was also observed for the whole range of impeller speed ratios tested. This fact was not so obvious. Indeed, the dual impeller speed has a strong impact on the homogenization process. One may note in Table 1 that mixing times (to achieve 90% homogeneity) determined experimentally vary between 30 and 160 s depending on impeller speed ratios.

Figure 6 is another representation which proves the validity of the model developed in this work to mimic mixing processes with planetary mixers. Indeed, we can observe that the volume of the perfect-mixed zone obtained by adjusting the model to the experimental data obeys Eq. 6.

All these results concerning modeling show us that it is possible to describe the mixing process which occurs with viscous fluids in a planetary mixer using the arrangement of reactors proposed. Moreover, the arrangement of ideal reactors proposed requires only the knowledge of one empirical parameter (the volume of the perfect-mixed zone). This empirical parameter can be easily obtained using preliminary experimental mixing runs.

Conclusion

In this work, an arrangement of ideal reactors containing a perfect-mixed zone sliding in a torus reactor is proposed to capture the dynamics of the mixing process with a planetary mixer involving highly viscous fluids. The originality of the arrangement of ideal reactors developed is due to the time-dependent location of the perfect-mixed zone in the torus which mimics the periodic revolution motion of the agitator around the vertical and central axis in the vessel.

The arrangement of ideal reactors proposed requires only the knowledge of a unique parameter: the volume of the perfect-mixed zone. This parameter can be easily obtained using preliminary experimental mixing runs. A method based on colorimetric diagnosis has been applied to identify it and to establish its dependence with impeller rotational speed.

It is shown that for a given agitated fluid and mixing system, modeling results are in close agreement with experimental ones on the whole range of impeller speeds ratio tested which shows that the model proposed captures well the physical mixing phenomena.

There is no limitation for predicting the dynamics of the mixing processes of other planetary mixers with such model arrangements; only identification parts should be reiterated.

Literature Cited

1. Danckwerts PV. Continuous flow systems. Distribution of residence times. *Chem Eng Sci*. 1953;2:1–13.
2. Dieulot JY, Petit N, Rouchon P, Delaplace G. An arrangement of ideal zones with shifting boundaries as away to model mixing processes in unsteady stirring conditions in agitated vessels. *Chem Eng Sci*. 2005;60:5544–5554.
3. Tanguy PA, Thibault F, Dubois C, Aït-Kadi A. Mixing hydrodynamics in a double planetary mixer. *Trans Inst Chem Eng*. 1999;77:318–323.
4. Tanguy PA, Bertrand F, Labrie R, Brito de la Fuente E. Numerical modelling of the mixing of viscoplastic slurries in a twin blade planetary mixer. *Trans Inst Chem Eng*. 1996;74:499–504.
5. Landin M, York P, Cliff,MJ, Rowe RC. Scale up of a pharmaceutical granulation in planetary mixers. *Pharm Dev Technol*. 1999;4:145–150.
6. Jongen T. Characterization of batch mixers using numerical flow simulations. *AIChE J*. 2000;46:2140–2150.
7. Zhou G, Tanguy PA, Dubois C. Power consumption in a double planetary mixer with non-Newtonian and viscoelastic material. *Trans Inst Chem Eng*. 2000;78:445–453.
8. Delaplace G, Guérin R, Leuliet JC. Dimensional analysis for planetary mixer: modified power and Reynolds numbers. *AIChE J*. 2005;51:3094–3100.
9. Delaplace G, Bouvier L, Moreau A, Guérin R, Leuliet JC. Determination of mixing time by colourimetric diagnosis-application to a new mixing system. *Exp Fluids*. 2004;36:437–443.
10. Delaplace G, Thakur RK, Bouvier L, André C, Torrez C. Dimensional analysis for planetary mixer: mixing time and Reynolds numbers. *Chem Eng Sci*. 2007;62:1442–1447.
11. Chhabra RP, Bouvier L, Cuvelier G, Domenek S, André C, Delaplace G. Determination of mixing times with helical ribbon impeller for non-Newtonian viscous fluids using an advanced imaging method. *Chem Eng Technol*. 2007;30:1686–1691.
12. Cabaret F, Fradette L, Tanguy PA. Characterization of macromixing kinetics using advanced image analysis. *Proceeding of 12th European Conference on Mixing*, Bologna, Italy, 2006:391–398.

Appendix

Whatever the interval of time, the torus reactor is constituted by n compartments and can be regarded as a vector of n rows.

For a given step of time, the torus reactor is constituted by two types of compartments: those which are overlapped

by the perfect-mixed zone and the others constituting the perfect-mixed zone. The number of compartments which are not overlapped by the perfect-mixed zone correspond to a vector of $(n - n_{\mathrm{mix}})$ rows. This vector is: C_{adj_p} with $1 \leq p \leq (n - n_{\mathrm{mix}})$.The first row of this vector C_{adj_1} corresponds to the cell which is adjacent and located in the forehead of the perfect-mixed zone.

To know the evolution of spatial concentration in the torus reactor, it is necessary to update mass balance between two consecutive intervals of time to predict the values of the two vectors constituting the torus reactor.

Introducing C_k as the tracer concentration in the kth compartment at the initial time (injection) and $(j \cdot \Delta t)$ as the jth interval of time, it can be shown that for the first time steps, $1 \leq j < n - n_{\mathrm{mix}} + 1$:

$$C_{\mathrm{adj}_p}((J-1).\Delta t) = C_k \quad \text{with}$$

$$k = (n_{\mathrm{mix}} + 1) + (j-1) + (p-1) - n.Ent\left(\frac{n_{\mathrm{mix}} + (J-1) + (p-1)}{n}\right) \quad \text{and}$$

with $1 \leq p \leq (n - n_{\mathrm{mix}})$.

For higher time steps, $j \geq n - n_{\mathrm{mix}} + 1$, the compartments constituting the adjacent vector C_{adj_p} have been previously swept out by the perfect-mixed zone and consequently it can be shown,

$$C_{\mathrm{adj}_p}((J-1).\Delta t) = C_{\mathrm{mixed\ zone}}(((J-1) + (p-1) - (n - n_{\mathrm{mix}})).\Delta t) \text{ with } 1 \leq p \leq (n - n_{\mathrm{mix}})$$

The concentration in each compartment constituting the perfect-mixed zone are all equal and consequently it can be shown by a tracer mass balance at a step of time $(j \cdot \Delta t)$ $(j \geq 1)$ is:

$$C_{\mathrm{mixed\ zone}}(J.\Delta t) = \frac{(n_{\mathrm{mix}} - 1).C_{\mathrm{mixed\ zone}}((J-1).\Delta t) + C_{\mathrm{adj}_1}((J-1).\Delta t)}{n_{\mathrm{mix}}}$$

$C_{\mathrm{adj}_1}((J-1).\Delta t)$ is the concentration reached in the adjacent cell to the forehead of the perfect-mixed zone at time $(J - 1)\Delta t$ and $C_{\mathrm{mixed\ zone}}(0) = C_k$ with $1 \leq k \leq n_{\mathrm{mix}}$.

Manuscript received Jun. 12, 2009, revision received Apr. 26, 2010, and final revision received July 16, 2010.